Technoeconomic Optimization of Continuous Crystallization for Three Active Pharmaceutical Ingredients: Cyclosporine, Paracetamol, and Aliskiren

Technoeconomic Optimization of Continuous Crystallization for Three Active Pharmaceutical Ingredients (APIs): Cyclosporine, Paracetamol and Aliskiren

Samir Diab, Dimitrios I. Gerogiorgis*

School of Engineering (IMP), University of Edinburgh, The King's Buildings, Edinburgh, EH9 3FB, Scotland, United Kingdom (UK)

**Corresponding Author*: D.Gerogiorgis@ed.ac.uk (*+44 131 6517072*)

ABSTRACT

Mixed Suspension-Mixed Product Removal (MSMPR) crystallizers are widely implemented for the continuous crystallization of active pharmaceutical ingredients (APIs), allowing enhanced efficiency, flexibility and product quality compared to the currently dominant batch crystallizer designs. Establishing cost-effective continuous crystallization process configurations for societally- and economically-important APIs is essential to ensure the successful implementation of fully end-to-end continuous pharmaceutical manufacturing (CPM) campaigns. Process modelling and optimization allow rapid, systematic comparison of technoeconomic evaluations. This paper pursues total cost minimization of different crystallizer configurations of three APIs, cyclosporine, paracetamol and aliskiren hemifumarate, whose continuous MSMPR crystallization has been experimentally demonstrated. Nonlinear optimization for total cost configuration is implemented for 1-3 crystallizers for different plant API capacities with crystallizer temperatures and residence times as decision variables. Optimization results show that the optimal number of crystallizers is dependent on plant capacity; implementing one crystallizer is preferred for all three APIs at 10^2 kg y^{-1}, whilst multiple crystallizer implementation is more cost-beneficial at increased capacities. These trends are observed due to the increasing dominance of operating expenditures on total costs at increased capacities, making the benefits of implementing more crystallizers (enhanced yields, reduced utility loads) worth the increased capital expenditures. Process modelling and optimization allows rapid technoeconomic evaluation of MSMPR crystallizer configurations for different APIs towards systematic selection of optimal continuous crystallizer designs for pharmaceutical manufacturing.

1. Introduction

Continuous pharmaceutical manufacturing (CPM) has received significant attention from academia, industry and regulatory bodies[1] due to its potential for significant operational[2] and economic[3] benefits in comparison to traditionally implemented batch methods.[4] The wide variety of continuous flow synthetic route demonstrations[5–9] and integrated end-to-end CPM processes being implemented for pilot plant,[10] portable reconfigurable units[11] and production level processes[12,13] shows the beginning of the transition from batch to CPM in industry. While continuous flow syntheses of promising active pharmaceutical ingredients (APIs) are the foundation of CPM, establishing reliable continuous separation processes is paramount for successful end-to-end continuous manufacturing.[14]

A significant portion of pharmaceutical products are sold as solids (tablets, dispersions, gels or topical treatments), and thus crystallization is an essential unit operation in drug product manufacturing. Traditional batch crystallization techniques are widely studied and well understood, but batch-to-batch variability may induce deviations from product specifications regarding crystal product quality attributes, which leads to significant quantities of waste.[15] Continuous crystallization has received attention for its potential to increase flexibility, efficiency and quality.[16]

The mixed suspension, mixed product removal (MSMPR) crystallizer is a widely studied continuous crystallizer design due to its simple operation, low maintenance requirements, avoidance of rapid fouling typical of continuous solids processes and tubular crystallizer designs[17] and ease of adaptation from existing batch stirred tanks.[16] Recent work using MSMPRs for crystallization kinetic parameter estimation,[18–21] comparison of operating strategies, process configurations and control,[22–34] novel crystallization techniques,[35–38] specialized separations[39–46] and polymorph selectivity[47,48] have significantly developed MSMPR implementation, with some designs integrated into end-to-end CPM plants.[10,49] However, continuous crystallizer designs operate at steady-state and thus do not reach equilibrium, leading to potentially lower yields compared to batch processes; establishing technically feasible and economically viable operating parameters for continuous designs is essential for the successful transition from batch to continuous crystallization methods.

Investigation of continuous processes for APIs of economic significance to the pharmaceutical industry is important to realize the technoeconomic benefits attainable via CPM. Several pharmaceutical compounds have been investigated for their MSMPR crystallization in the literature, including the APIs: cyclosporine, an immunosuppressant with applications for skin ailment treatment (namely psoriasis) and rheumatoid arthritis, paracetamol, the popular analgesic, and aliskiren hemifumarate, a renin inhibitor for the treatment of primary hypertension. Historic and predicted revenues for prescription hypertensive[50] and non-prescription analgesics and skin treatment medicines[51] (Figure 1) and their multiple formulation types (Table 1) illustrate the societal and economic importance of these APIs in the pharmaceutical industry. The optimal design of continuous crystallization processes for their integration into CPM campaigns is paramount.

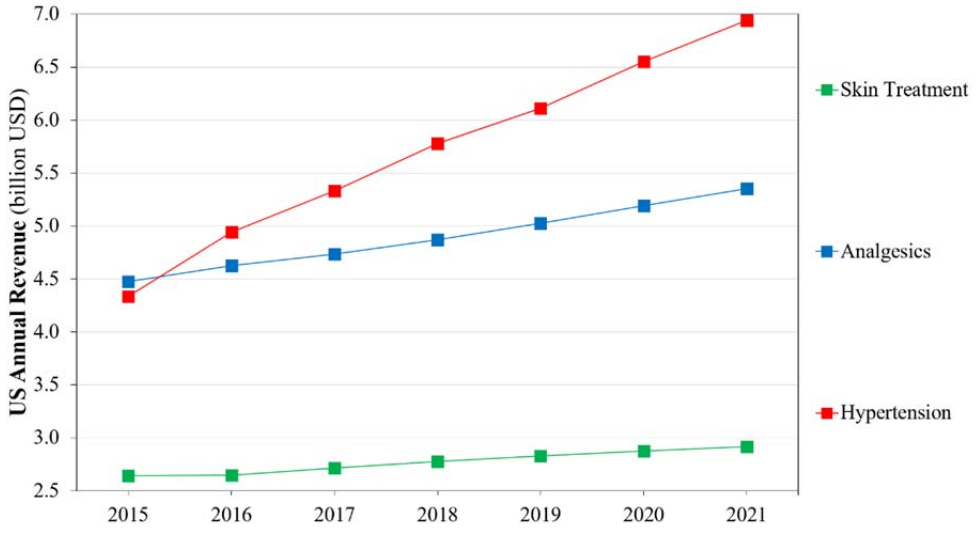

Figure 1: Historical and predicted US revenues for prescription hypertension (aliskiren) and non-prescription analgesic (paracetamol) and skin treatment (cyclosporine, psoriasis) drugs.

Table 1: Brands and formulations of cyclosporine, paracetamol and aliskiren.

API	Application	Brand Name	Prescription?	Patented?	Formulation
Cyclosporine	Immunosuppressant	Sandimmune®	✓	✓	Oral capsule Oral solution Intravenous solution
		Cicloral®	✓	X	Oral capsule
		Deximune®	✓	X	Oral capsule
	Psoriasis	Neoral®	✓	✓	Oral capsule Oral solution
	Rheumatoid arthritis	Neoral®	✓	✓	Oral capsule Oral solution
	Keratoconjunctivitis	Restasis®	✓	✓	Ophthalmic emulsion
Paracetamol[a]	Analgaesic	Tylenol®	X	X	Oral tablet
		Calpol®	X	X	Oral suspension
		Panadol®	X	X	Oral tablet
Aliskiren	Hypertension	Tekturna®	✓	✓	Oral tablet
		Rasilez®	✓	✓	Oral tablet

Continuous crystallization design must be cost-effective; while various studies have optimized MSMPR configurations to maximize yield and purity, technoeconomic optimization to establish viable MSMPR process configurations has yet to be widely conducted.[52–55] Process modelling and optimization are useful tools for rapid technoeconomic evaluations of candidate designs;[56] doing so for societally important APIs with high sales volumes is essential for successful demonstration of continuous crystallizer configurations prior to pilot plant implementation and scale up.

This work conducts total cost minimization by nonlinear optimization of different MSMPR cascades for cyclosporine, paracetamol and aliskiren hemifumarate. First, we describe the continuous crystallization process implemented for all three APIs. Subsequently, we describe the process model, costing methodology and the constrained nonlinear optimization problem formulation for total cost minimization. We then present minimal total cost components for all APIs for varying numbers of crystallizers and different plant API capacities with corresponding optimal design parameters of the implemented crystallizers.

2. Process Modelling and Nonlinear Optimization Methodology

2.1 Process Flowsheet

The process investigated here is the continuous MSMPR crystallization of cyclosporine, paracetamol and aliskiren (hemifumarate), whose relevant physical properties are listed in Table 2. The process flowsheet for a cascade of MSMPR crystallizers in series for continuous crystallization based on experimental demonstrations[19,20,38] is shown in Figure 2. A mother liquor stream containing dissolved API enters the first crystallizer, whose product magma is the feed stream to the subsequent crystallizer in the cascade. Crystallization occurs by cooling only, without the need for an antisolvent to generate supersaturation.[19,20,38] Experimental setups for the MSMPR crystallization of cyclosporine, paracetamol and aliskiren have shown that configurations with no recycle are efficient in terms of both yield and purity. MSMPR studies investigating mother liquor recycle options for cyclosporine showed that increasing recycle ratios lead to increasing accumulation of impurity in the crystalline product. Solids recycle options for the MSMPR crystallization of cyclosporine[24] were shown to be economically inferior to those without recycle due to significant API losses in purge streams required to maintain steady-state operation, which had a detrimental effect on plantwide API yield and total costs.[57] Throughout this study, we model a series of MSMPR crystallizers without recycle (Figure 2).

Cyclosporine is crystallized by cooling from a mother liquor solvent of acetone;[38] paracetamol is crystallized from a 4:1 mixture (volume basis) of isopropanol:water;[19] aliskiren hemifumarate is crystallized from a 1:1 mixture of ethyl acetate:ethanol (mass basis).[20] The experimental demonstration of aliskiren hemifumarate crystallization describes a reactive crystallization step performed at 20 °C prior to cooling crystallization,[20] which is assumed to be conducted prior to the process considered here. The cascade consists of N = 1-3 crystallizers. We consider plant API

capacities (Q_{API}) of 10^2, 10^3 and 10^4 kg API per year to investigate the effects of production scale, which can significantly affect the economic viability of modelled CPM designs.[58] Varying design capacities (Q_{API}) considered here do not signify a range of capacities implemented for a single plant; they are considered for separate plant designs to comparatively illustrate the effect of capacity on relevant cost components and their relative contribution to total plant costs. The considered plant capacities, $Q_{API} = \{10^2, 10^3, 10^4\}$ kg API y^{-1} are justified since continuous processing technologies are yet to be widely implemented in pharmaceutical manufacturing, hence a CPM process may first be implemented at a rather small production scale, beyond the published literature demonstration cases. Three different capacities have been compared here for each API, to illustrate the effect of capacity on cost-optimal design and operating parameters, and its relative influence on individual category contributions to total cost. For the considered plant capacities, $Q_{API} = \{10^2, 10^3, 10^4\}$ kg API y^{-1}, we explore the effect of allowing one, two and three MSMPR crystallizers for CPM implementation, a range consistent with our recently published study.[57] Crystallizer operating temperatures are between –10 and 20 °C, and the maximum total cascade residence is 15 h. Concentrations of dissolved API in mother liquor feed streams (C_0) vary according to experimental procedures;[19,20,38] cyclosporine, paracetamol and aliskiren feed concentrations of 25, 8.86 and 6% w/w, respectively, are assumed.

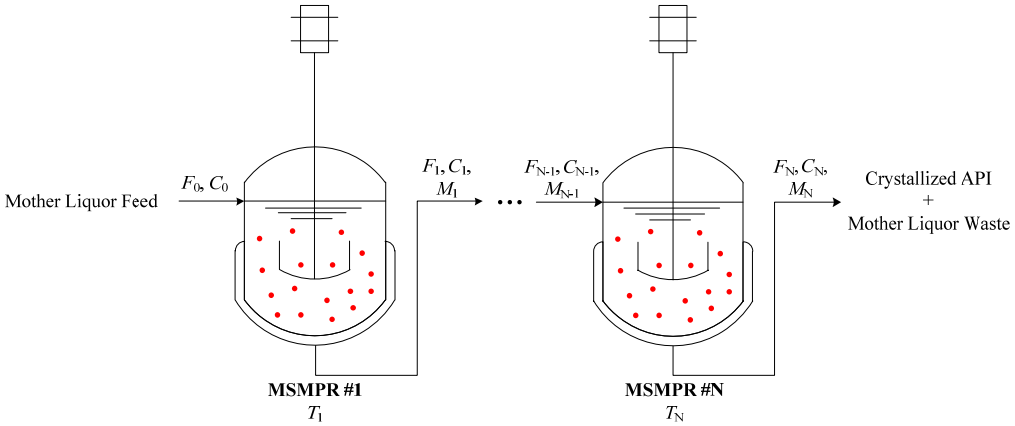

Figure 2: Process flowsheet of a cascade of continuous MSMPR crystallizers.

This work considers MSMPR cascades for continuous cooling crystallization with no antisolvent usage, recycle implementation or up-/downstream requirements considered to affect the process. In practice, distribution of impurities from upstream unit operations is an important consideration in crystallization operating parameter selection and its effects on downstream processing requirements. We assume that fresh mother liquor feed streams contain negligible amounts of impurity that will affect the attained crystal purities in these processes, due to uncertainties in crystallization feed stream compositions. Knowledge of typical crystallization feed stream compositions in integrated CPM processes will greatly enhance the understanding of impurity distributions on optimal continuous crystallization process designs for the APIs studied here.

Table 2: Physical properties of cyclosporine, paracetamol and aliskiren.

API	Formula	CAS #	MW ($g\ mol^{-1}$)	Density, ρ_{API} ($g\ mL^{-1}$)	Melting Point (°C)
Cyclosporine	$C_{62}H_{111}N_{11}O_{12}$	59865-13-3	1,206.61	1.30	150
Paracetamol	$C_8H_9NO_2$	103-90-2	151.16	1.33	169
Aliskiren	$C_{30}H_{55}N_3O_6$	173334-57-1	551.76	1.20	99

2.2 Steady-State Process Model

MSMPR crystallization assumes a clear, homogeneous feed mother liquor stream containing no crystals. All crystallizers operate at steady-state; product magmas exit all crystallizers at equilibrium and have the same composition as the crystallizer contents (i.e., crystallizer contents are perfectly mixed). No crystal breakage or attrition occurs and crystal growth is assumed linear (one-dimensional) and size-independent. The steady-state process model describes crystallisation kinetics,

API solubilities, crystal population balances and process mass balances; the simultaneous solution of these equations describes continuous MSMPR crystallization. The model is solved in MATLAB, implementing the same methodology and solver settings as described in our previous publication.[57]

2.2.1 Crystallization Kinetics

Crystal growth and nucleation kinetics are described by Arrhenius-type power law expressions.

$$G_i = k_{g0} \exp\left(-\frac{E_{ag}}{R(T_i + 273.15)}\right)\left(\frac{C_i}{C_i^{sat}} - 1\right)^g \quad (1)$$

$$B_i = k_{b0} \exp\left(-\frac{E_{ab}}{R(T_i + 273.15)}\right)\left(\frac{C_i}{C_i^{sat}} - 1\right)^b M_i^m \quad (2)$$

Here, G_i and B_i are the crystal growth and nucleation rates in MSMPR i operating at temperature T_i, respectively. C_i and $C_{sat,i}$ are the API equilibrium (outlet) and saturation (solubility) concentrations at T_i, respectively. M_i is the slurry density in MSMPR i. Growth kinetic parameters are k_{g0}, the growth pre-exponential factor, E_{ag}, the growth energy barrier, and g, the growth exponent. Nucleation parameters are k_{b0}, the nucleation pre-exponential factor, E_{ab}, the nucleation energy barrier, b, the nucleation exponent, and m, the slurry density exponent. Temperature-dependency of crystal nucleation for paracetamol and aliskiren has not been considered in the literature,[19,20] and thus E_{ab} for these APIs equals zero. Similarly, m for aliskiren is considered equal to zero.[20] The units of k_{b0} for paracetamol available in the literature are not consistent with the developed process model,[57] so the value of B_i for paracetamol crystallization processes must be converted from mass- to volume-based units. Crystallization kinetic parameters from the literature for all APIs are summarized in Table 3.

Table 3: Steady-state process model parameters for continuous MSMPR crystallization.

API	Cyclosporine ($C_{62}H_{111}N_{11}O_{12}$)		Paracetamol ($C_8H_9NO_2$)		Aliskiren ($C_{30}H_{55}N_3O_6$)	
	Value	Units	Value	Units	Value	Units
k_{g0}	$1.13 \cdot 10^7$	m min^{-1}	$2.00 \cdot 10^{-2}$	m min^{-1}	$2.9 \cdot 10^{-4}$	m min^{-1}
E_{ag}/R	$9.06 \cdot 10^3$	K	$1.73 \cdot 10^3$	K	$3.5 \cdot 10^2$	K
g	1.33	–	1.08	–	1.08	–
k_{b0}	$4.80 \cdot 10^{20}$	# crystals m^{-3} min^{-1}	295	# crystals kg^{-1} s^{-1}	$3.2 \cdot 10^7$	# crystals m^{-3} min^{-1}
E_{ab}/R	$7.03 \cdot 10^3$	K	0	K	0	K
b	1.50	–	2.14	–	1.95	–
m	2/3	–	1.62	–	0	–
k_v	$\pi/6$	–	0.61	–	0.04	–

Solubilities of APIs (i.e., API saturation concentrations, $C_{sat,i}$) as a function of temperature are required for accurate description of crystallization kinetics. Saturation concentrations as a function of temperature are described as temperature-dependent polynomials regressed from experimental solubility data for cyclosporine,[31,57] paracetamol,[19] and aliskiren.[20]

$$C_{i,sat} = (1.17 \cdot 10^{-4})T_i^2 + (2.00 \cdot 10^{-4})T_i + 0.05 \quad \text{for} \quad (3)$$

$$C_{i,sat} = (3.79 \cdot 10^{-2})T_i^2 + (3.77 \cdot 10^{-1})T_i + 0.21 \quad \text{for paracetamol} \quad (4)$$

$$C_{i,sat} = (7.60 \cdot 10^{-7})T_i^3 - (3.20 \cdot 10^{-5})T_i^2 + (5.20 \cdot 10^{-4})T_i + (4.50 \cdot 10^{-3}) \quad \text{for aliskiren} \quad (5)$$

2.2.2 Population Balance Equations

The general one-dimensional population balance model is described by a system of ordinary differential equations (ODEs).

$$G_1 V_1 \frac{dn_1}{dL} = -F_1 n_1 \quad (6)$$

$$G_i V_i \frac{dn_i}{dL} = F_{i-1} n_{i-1} - F_i n_i \qquad i = 2 \ldots N. \quad (7)$$

V_i is the volume of MSMPR i, F_{i-1} and F_i are the volumetric flowrates of streams entering and leaving MSMPR i, respectively (Figure 2), N is the number of crystallizers in the cascade, n_i is the crystal population density and L is the characteristic (one-dimensional) length of the crystal. Population balance equations are satisfied by the boundary condition $n_i^0 = n_i(L = 0)$, corresponding to the crystal nuclei population density.

$$n_i^0 = \frac{B_i}{G_i} \tag{8}$$

The slurry density, M_i, is calculated from the population density (eq. 9).

$$M_i = k_v \rho_{API} \int n_i L^3 \mathrm{d}L \tag{9}$$

k_v is the crystal volume shape factor[59–61] and ρ_{API} is the API crystal density; values for all APIs are listed in Tables 2 and 3.

2.2.3 Process Mass Balances

The steady-state mass balances for each process assume no material accumulation and account for volumetric changes due to solid formation due to API crystallization.

$$F_0 C_0 - F_1 \left(1 - \frac{M_1}{\rho_{API}}\right) C_1 - F_1 M_1 = 0 \tag{10}$$

$$F_{i-1} \left(1 - \frac{M_{i-1}}{\rho_{API}}\right) C_{i-1} + F_{i-1} M_{i-1} - F_i \left(1 - \frac{M_i}{\rho_{API}}\right) C_i - F_i M_i = 0 \qquad i = 2 \ldots N. \tag{11}$$

F_0 and C_0 are the fresh feed volumetric flowrate and mother liquor API concentration to the first crystallizer, respectively. An API balance across mother liquor and crystallised solid phases also gives the following expression for the slurry density from the process mass balances.

$$M_i = C_{i-1} - C_i \tag{12}$$

2.2.4 Crystallization Yield

The crystallization yield is calculated from the mother liquor API concentration exiting the final crystallizer relative to the API concentration in the feed stream to the first crystallizer.

$$Y_{cryst} = 100 \left(1 - \frac{C_N}{C_0}\right) \tag{13}$$

2.2.5 Crystallizer Volumes

Crystallizer volumes are calculated from the specified residence time (τ_i) and the volumetric flowrate through the crystallizer.

$$V_i = F_i \tau_i \tag{14}$$

2.2.6 Costing Methodology

We implement an established methodology for costing pharmaceutical manufacturing processes.[3] All crystallization cascade designs are assumed to be implemented at an existing pharmaceutical manufacturing site with essential auxiliary structures already in place; for the capacities considered here ($Q_{API} = 10^2, 10^3, 10^4$ kg API y^{-1}), construction of a dedicated facility is unlikely, and so this is a reasonable assumption. Annual operation of 8,000 hours is considered.

Prices for equipment of similar capacities to those considered here have been sourced where possible; where such data is unavailable, the following cost-capacity correlation is used.[62]

$$P_B = f P_A \left(\frac{S_B}{S_A}\right)^n \tag{15}$$

P_j is the equipment purchase cost at capacity S_j. Parameters n and f are equipment-dependent and can be found in the literature.[63] Wherever the reference purchase cost (P_A) is taken from the past, chemical engineering plant cost indices (CEPCIs) are used to calculate the corresponding present purchase cost in the present day. All equipment capacities are scaled to account for plantwide inefficiencies to meet

the specified plant capacity. Table 4 gives details for the purchase costs and scaling parameters in eq. 15 for each equipment item.

Table 4: Equipment parameters for calculating scaled equipment purchase costs in the present day (eq. 15).

Item	Ref. Year	Ref. Cost, P_A (GBP)	Capacity Basis	Ref. Capacity, S_A	n	f (%)	Ref.
Crystallizer	2007	328,875	m^3	3.00	0.53	10.33	([61])
Pump	2015	958	–	–	1.00	–	([62])
Cooler	2007	3,454	–	–	1.00	–	([61])

The sum of all inflation-adjusted equipment costs (P_B) gives the Free-on-Board (FOB) cost. The Chilton method is used to calculate the Battery Limits Installed Cost (BLIC).[64] The installed equipment cost (IEC), process piping and instrumentation (PPI) and total physical plant cost (TPPC) are calculated from eqs. 16-18. A construction factor of 30% is added to TPPC to calculate the BLIC (eq. 19).[3]

$$\text{IEC} = 1.43\text{FOB} \tag{16}$$

$$\text{PPI} = 0.42\text{IEC} \tag{17}$$

$$\text{TPPC} = \text{IEC} + \text{PPI} \tag{18}$$

$$\text{BLIC} = 1.3\text{TPPC} \tag{19}$$

Working capital and contingency costs (WCC) are calculated as follows. Working capital (WC) costs are taken as 3.5% of annual material (mother liquor solvent) costs ($\text{MAT}_{\text{annual}}$).[3] Contingency costs (CC) are calculated as 20% of the BLIC. The sum of BLIC and WCC gives the total capital expenditure (CapEx).

$$\text{WC} = 0.035\text{MAT}_{\text{annual}} \tag{20}$$

$$\text{CC} = 0.2\text{BLIC} \tag{21}$$

$$\text{WCC} = \text{WC} + \text{CC} \tag{22}$$

$$\text{CapEx} = \text{BLIC} + \text{WCC} \tag{23}$$

Material prices are sourced from various vendors and are summarised in Table 4. The annual utilities cost ($\text{UTIL}_{\text{annual}}$) is calculated as 0.96 GBP kg^{-1} of material input; the annual waste cost ($\text{Waste}_{\text{annual}}$) is 0.35 GBP L^{-1} of waste produced.[3] Annual operating expenditure ($\text{OpEx}_{\text{annual}}$) is calculated as the sum of annual material ($\text{MAT}_{\text{annual}}$), utilities ($\text{UTIL}_{\text{annual}}$) and waste disposal ($\text{Waste}_{\text{annual}}$). Here, ρ_{solvent} is the mother liquor solvent (Table 5). Labour costs are not considered here due to the small scale of production and automated nature of continuous operation.

$$\text{UTIL}_{\text{annual}} = 0.96F_0\left(\rho_{\text{solvent}} + C_0\right) \tag{24}$$

$$\text{Waste}_{\text{annual}} = 0.35F_{\text{N}} \tag{25}$$

$$\text{OpEx}_{\text{annual}} = \text{MAT}_{\text{annual}} + \text{UTIL}_{\text{annual}} + \text{Waste}_{\text{annual}} \tag{26}$$

The total cost of the plant designs is calculated as the sum of CapEx and the sum inflation-adjusted $\text{OpEx}_{\text{annual}}$ over the plant lifetime.

$$\text{Total Cost} = \text{CapEx} + \sum_{k=1}^{t} \frac{\text{OpEx}_{\text{annual}}}{(1+r)^{\text{k}}} \tag{27}$$

A plant-operating lifetime (t) of 20 years and an interest rate (r, accounting for inflation) of 5% are considered. All CapEx is assumed to occur in year 0 and operation is assumed to begin in year 1.

Table 5: Material prices of mother liquor solvents for each API continuous crystallization process.

API	**Material** (mother liquor solvent)	**Material Cost** (GBP kg^{-1})
Cyclosporine	Acetone	0.29
Paracetamol	Isopropanol	0.29
	Water	0.60
Aliskiren	Ethyl Acetate	0.56
	Ethanol	0.61

2.2.7 Nonlinear Optimization Formulation

The objective function (eq. 28) of the nonlinear optimization problem is the total cost (eq. 27). The decision variables are the residence time and temperature of each crystallizer in the cascade, both of which affect the final attainable crystallization yield, process mass balances and total costs of the cascade design. Crystallization temperatures are constrained between -10 and 20 °C and the temperature of each crystallizer must be lower than or equal to the previous (eq. 29). Crystallizers of equal residence times are assumed for the problem formulation (eq. 30). Implementing crystallizers of equal volumes makes their purchase and acquirement from equipment suppliers/manufacturers simpler and less expensive. Additionally, the total cascade residence time is allowed a maximum of 15 h (eq. 31) in accordance with our previous work.[57]

$$\min \text{Total Cost} \tag{28}$$

$$-10\ °C \leq T_N \leq \ldots \leq T_1 \leq 20\ °C \tag{29}$$

$$\tau_1 = \ldots = \tau_N \tag{30}$$

$$\sum_{i=1}^{N} \tau_i \leq 15\ h \tag{31}$$

The optimization problem is solved in MATLAB using the built-in solver fmincon, implementing the (default) interior-point algorithm with tolerances of 10^{-6}. The problem was solved separately for all combinations of API = {cyclosporine, paracetamol, aliskiren}, number of implemented crystallizers, N = {1, 2, 3}, and plant capacity, Q_{API} = {10^2, 10^3, 10^4} kg API per annum, i.e., 9 problem instances in total, to avoid mixed integer problem formulations, which would increase the computational effort.

Multiple initial values for decision variables have been used to ensure a unique optimal solution for each problem instance. The temperature and residence time of each crystallizer in series are the decision variables of the nonlinear optimization problem; thus, the number of decision variables for configurations consisting of N crystallizers = $2N$. Table 6 shows the combinations of starting points used for varying numbers of crystallizers for each API and considered plant capacity. Each problem instance resulted in a unique solution, independent of the starting point.

Table 6: Decision variable initial values for and plant capacities for different numbers of crystallizers (N).

N	Decision Variable	Initial Value	No. points, $\boldsymbol{T_0} \times \boldsymbol{\tau_0}$
1	$\boldsymbol{T_0} = T_{1,0}$ (°C)	{ -5 , 0 , 5 }	9
	$\boldsymbol{\tau_0} = \tau_{1,0}$ (h)	{ 3 , 8 , 13 }	
2	$\boldsymbol{T_0} = [T_1, T_2]_0$ (°C)	{ [-5,-5] , [0,-5] , [10,5] , [15,15] }	20
	$\boldsymbol{\tau_0} = [\tau_1, \tau_2]_0$ (h)	{ [3,3] , [3,6] , [3,9] , [6,3] , [9,3] }	
3	$\boldsymbol{T_0} = [T_1, T_2, T_3]_0$ (°C)	{ [-5,-5,-5] , [0,-5,-5] , [5,0,0] , [10,5,5] , [15,10,10] , [15,15,15] }	24
	$\boldsymbol{\tau_0} = [\tau_1, \tau_2, \tau_3]_0$ (h)	{ [3,3,3] , [3,3,6] , [3,6,3] , [6,3,3] }	

3. Results and Discussion

Total cost minimization via nonlinear optimization was implemented for each API (cyclosporine, paracetamol and aliskiren), for a varying number of crystallizers (N = 1, 2, 3) and plant capacity (Q_{API}

= 10^2, 10^3, 10^4 kg API y^{-1}). Minimum total cost components for all APIs for different numbers of implemented crystallizers and plant capacities are illustrated in Figure 3 and Tables S1-3 in the Supplementary Information.

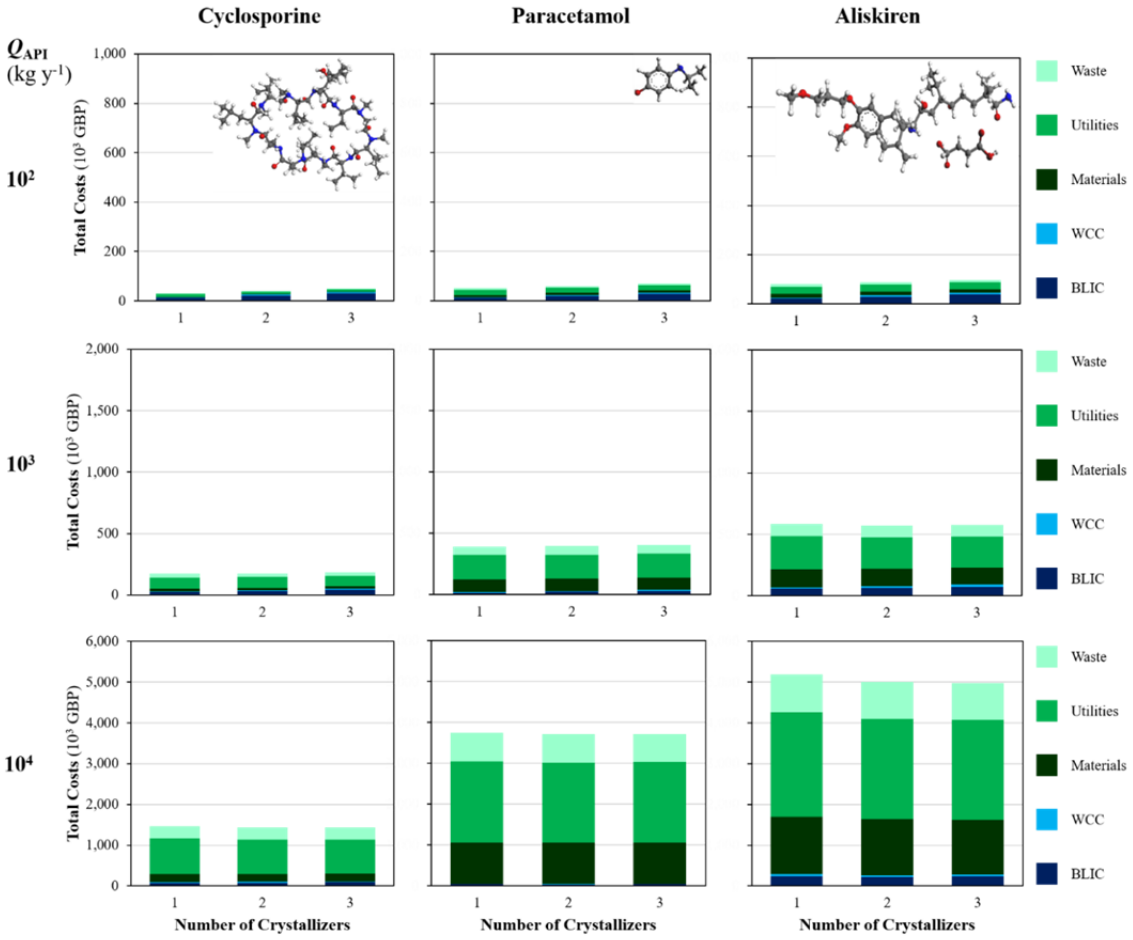

Figure 3: Minimum total cost components for each API at different plant capacities.

3.1 Capital Expenditures (CapEx)

Total CapEx increases with plant API capacity due to the need for larger crystallizer volumes to contain higher throughputs of crystallization magma. Figure 4 shows total cost components normalized with respect to total plant API capacity, which further illustrates the decreasing contribution of CapEx components to total costs. Total CapEx values are dominated by BLIC contributions due to the high cost of crystallization equipment (Table 4), and WCC contributions increase with plant capacity as it is a linear function of material requirements (eqs. 20 and 22). Both BLIC and WCC contributions increase with the number of implemented crystallizers, despite decreasing total crystallization volumes and material requirements. This is due to the cost of additional pumps and cooling equipment accompanying the crystallizer cascade for continuous operation. The nonlinear optimization formulation here is described to minimize total costs; if the formulations were to maximize profits or net present value (NPV), it is possible that longer residence times would be preferred. Formulating the objective function as NPV (for maximization) requires the estimation of product sales revenues. While API class sales trends have been historically increasing (Figure 1), future market sales variations of individual APIs and brands are unknown and cannot be accurately accounted for. For this reason, the objective is instead to minimize the plant total costs. Varying the objective function of an optimization problem can produce widely varying optimal design and operating parameters;[65] comparison of optimization results for different objective function formulations is also possible, assuming availability of reliable API and brand sales prices/projections.

Figure 5 illustrates optimal process configurations (i.e., crystallizer operating temperatures and residence times corresponding to total cost minima) for each API with different numbers of crystallizers and API capacities considered (also listed in Tables S4-6 in the Supplementary Information). Crystallizer volumes increase with plant capacity to accommodate increased material throughputs. Increasing the number of implemented crystallizers decreases the total crystallization volume required. MSMPR operation assumes perfectly mixed, homogeneous crystallizer magmas discharging at equilibrium, and thus the crystallizer operates at the exit concentration; implementing multiple crystallizers in series increases product concentrations and thus increases yields, which thus requires smaller crystallizers for a given API and plant capacity. Total residence times for aliskiren are long due to the slow crystallization kinetics of the API (and hence its suitability for MSMPR operation) in accordance with experimental demonstrations.[20]

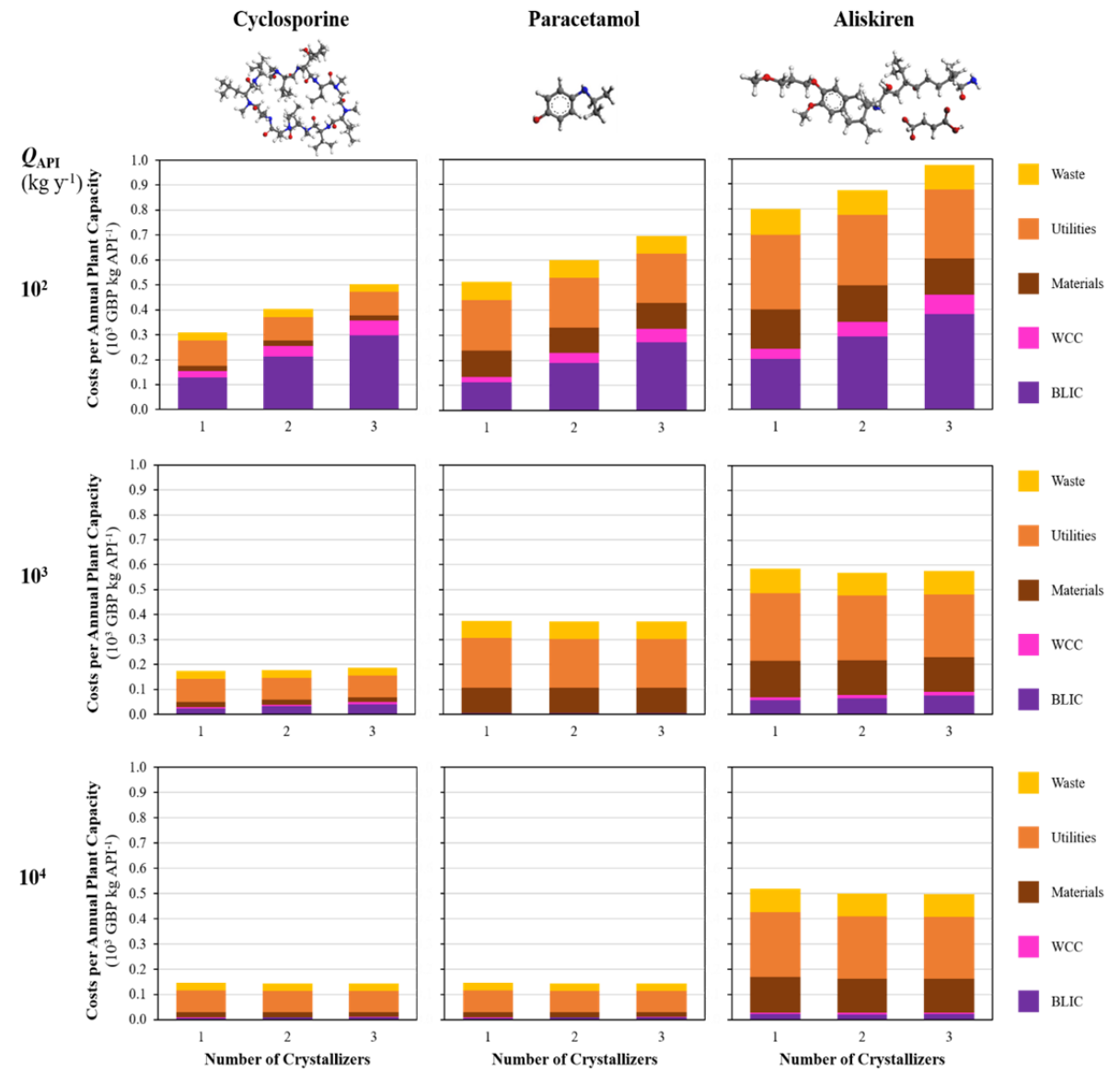

Figure 4: Minimum total cost components normalized with respect to plant capacity.

The equipment cost correlation used here is the most widely implemented and reliable available in the peer-reviewed literature. However, crystallizer design capacities (i.e., volumes) required for the considered plant capacities are at the lower end of the cost correlation application range, and thus purchase cost overestimation may be present. Additional uncertainty in calculated crystallizer purchase costs is present due to the lack of cost estimation methods for smaller crystallizer volumes

associated with lower plant capacities, e.g. cyclosporine at Q_{API} = 10^2 kg y^{-1} (Table S4 in the Supplementary Information); however, the cost correlation used here is the best available in the literature.

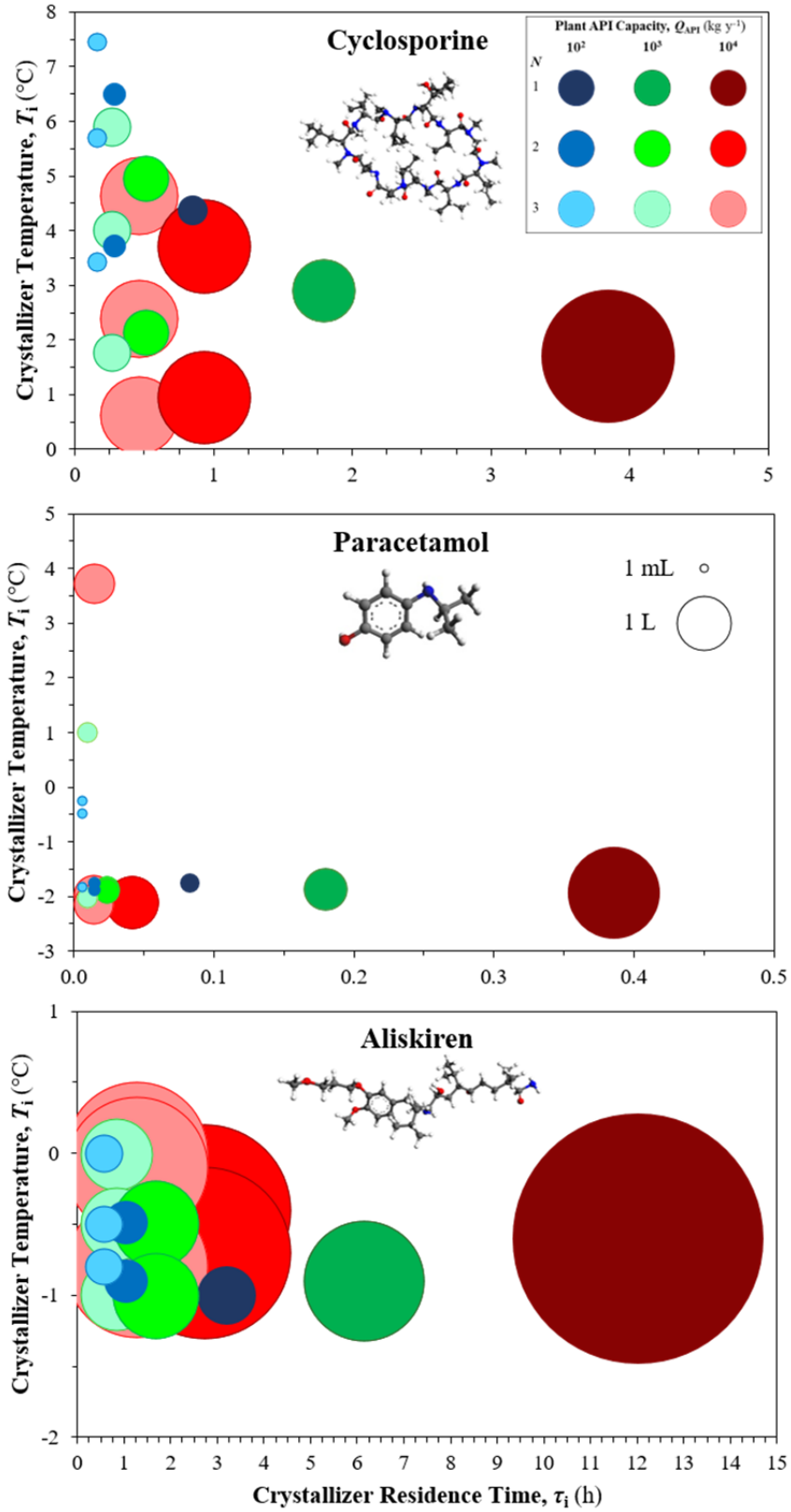

Figure 5: Crystallizer operating temperatures and residence times corresponding to total cost minima; bubble diameters are proportional to crystallizer volumes.

3.2 Operating Expenditures (OpEx)

Total OpEx increases with plant API capacity due to the higher required material throughputs and associated utilities and waste handling costs. Figure 6 shows the fractional relative minimum total cost component contributions for each API at varying plant capacities for one crystallizer. At lower API capacities, CapEx contributions are more significant; as plant capacity increases, OpEx component contributions become more significant, which is further illustrated by their continuing dominance over normalized CapEx components as plant API capacities increase (Figure 4). Utilities costs dominate OpEx contributions, however materials and waste handling costs become more significant with increasing plant capacity.

Cyclosporine operating temperatures are above zero and decrease along the crystallizer cascade (Figure 5 and Table S4 in the Supplementary Information), as described in the constrained nonlinear optimization constraints (eq. 29). Crystallizers for paracetamol and aliskiren also decrease in temperature along cascades, however operate at lower temperatures. In both cases, as the number of implemented crystallizers is increased, operating temperatures increase and residence times decrease; additional costs associated with increased cooling duties and larger crystallizers are not considered beneficial with respect to total costs. Rigorous temperature control via high-fidelity instrumentation can ensure designs remain at their optimal design parameters. The implementation of Process Analytical Technology (PAT) is essential for the success of CPM technologies, with recent studies illustrating its importance in crystallization applications.[66] Optimal crystallizer operating temperatures correspond to those required to attain minimum total costs of a design option; deviations from optimum design and operating parameters will lead to sub-optimal designs (i.e., higher total costs).

3.3 Total Costs

Minimum total costs for cyclosporine crystallization are attained when implementing one crystallizer only for API capacities of 10^2 and 10^3 kg API y^{-1} (Table S1 in the Supplementary Information); yield improvements associated with multiple crystallizer usage are only incremental (Table S4 in the Supplementary Information); thus, the associated additional BLIC costs are not beneficial. However, when the plant capacity is increased to 10^4 kg API y^{-1}, cyclosporine crystallization has lower total costs when two crystallizers are implemented. At higher capacities, OpEx components dominate total costs, and so even incremental increases in crystallization yield and distributed cooling loads across crystallizers can bring cost savings benefits.

For plant capacities of 10^2 and 10^3 kg API y^{-1}, paracetamol crystallization is cost optimal when implementing one crystallizer due to incremental yield improvements attainable with multiple crystallizer implementation at these capacities. Implementing two crystallizers is optimal at a plant capacity of 10^4 kg API y^{-1} (Table S2 in the Supplementary Information); this is due to the greater contribution of OpEx towards total costs at increased capacities as well as the reduced total crystallizer volume required (Table S5 in the Supplementary Information).

Continuous crystallization of aliskiren at a plant capacity of 10^2 kg API y^{-1} is cost optimal when implementing one crystallizer only; implementing two crystallizers at a capacity of 10^3 kg y^{-1} and three crystallizers at 10^4 kg y^{-1} is more cost effective (Table S3 in the Supplementary Information). The mother liquor solvent considered here (ethyl acetate:ethanol mixture) is more expensive than solvents for cyclosporine and paracetamol, thus material costs contribute more towards the dominant OpEx components (Table S6 in the Supplementary Information and Figure 6).

For the considered APIs and number of implementable crystallizers ($N = \{1, 2, 3\}$), multiple crystallizer usage is favoured as capacity increases. It is likely that there is some maximum number of crystallizers that allow minimum total costs for capacities beyond a certain value, however this cannot be stated with certainty from the results presented here; this can be clarified in future work. Total cost minimization at higher capacities can be investigated in the described modelling framework and methodology.

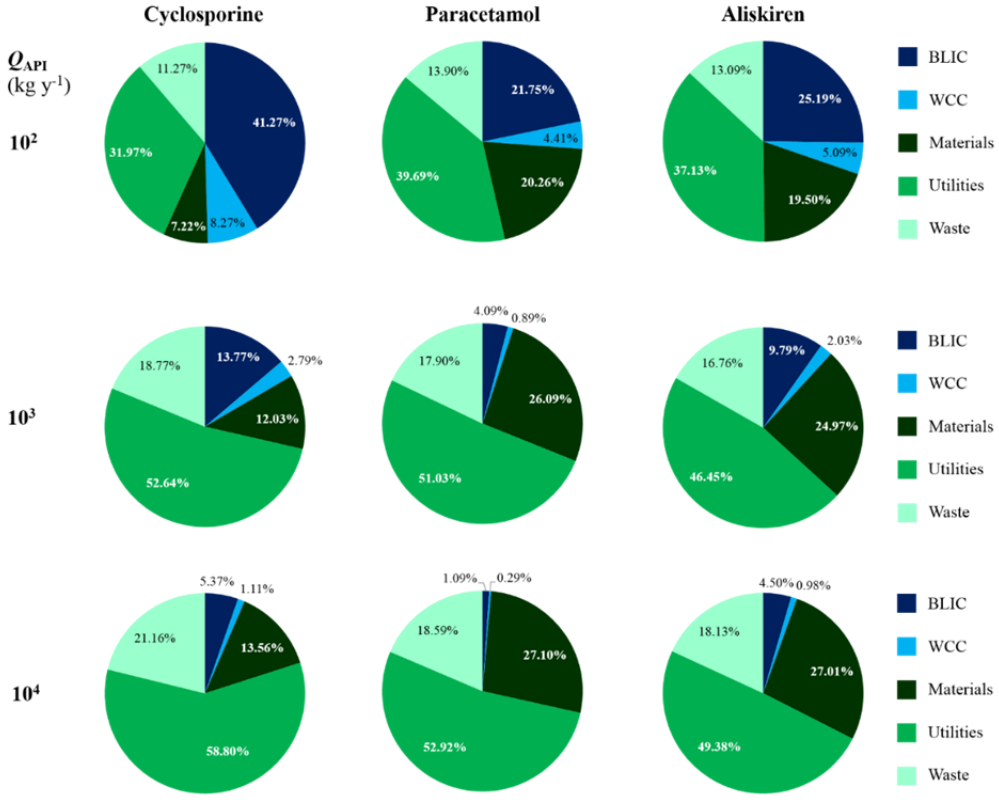

Figure 6: Component contributions towards total costs when implementing one crystallizer.

The relative effect of varying crystallization kinetics between the considered APIs varies with the plant capacity. For Q_{API} = 10^2 kg y^{-1}, cyclosporine CapEx components are significantly more dominant than at higher capacities for this API; material costs (OpEx) are less significant at lower capacities and thus the effect of cyclosporine's slow crystallization kinetics on CapEx (requiring longer residence times and crystallizer volumes) become more significant. CapEx component contributions for aliskiren are greater than those for paracetamol due to its slower crystallization kinetics. For both aliskiren and paracetamol, OpEx components are more significant even at Q_{API} = 10^2 kg y^{-1} as these APIs both require more expensive solvent components than cyclosporine (Table 5). The current modelling methodology and framework allows different APIs, capacities and numbers of implemented MSMPR crystallizers to be considered easily, given the availability of crystallization kinetic parameters and API temperature-dependent solubility data in a given mother liquor solvent system.

4. Conclusions

This work has conducted total cost minimization of continuous MSMPR crystallizer cascades for three societally and economically important APIs widely produced by the pharmaceutical industry: cyclosporine, paracetamol and aliskiren. Nonlinear optimization results show that the optimal number of crystallizers attaining minimal total costs is dependent on plant capacity. For the considered APIs, implementing one crystallizer is preferred at lower capacities, whilst multiple crystallizer usage is preferred at higher plant capacities. This result is observed due to the increasing dominance of operating expenditure contributions towards total costs at increased capacities, making the benefits of implementing more crystallizers (enhanced yields, reduced utility loads) worth the increased capital expenditure of purchasing multiple crystallization units. We have illustrated the value of conducting technoeconomic optimization studies such as this towards the development of continuous separations in pursuit of economically viable end-to-end CPM plants.

Associated Content

Supporting Information

Minimum total cost components and corresponding operating parameters and design variables for each API for different MSMPR design configurations. This information is available free of charge via the Internet at http://pubs.acs.org/.

Author Information

Corresponding Author

*Email: D.Gerogiorgis@ed.ac.uk , Phone : *+ 44 131 6517072*

ORCID

Dimitrios I. Gerogiorgis: 0000-0002-2210-6784

Notes

The authors declare no competing financial interest.

Acknowledgements

Mr. Samir Diab gratefully acknowledges the financial support of the Engineering and Physical Sciences Research Council (EPSRC) via a Doctoral Training partnership (DTP) PhD fellowship (Grant # EP/N509644/1). Moreover, Dr. D.I. Gerogiorgis acknowledges a Royal Academy of Engineering (RAEng) Industrial Fellowship. Tabulated and cited literature data suffice for reproduction of all original process simulation and optimisation results, and no other supporting data are required to ensure reproducibility.

Nomenclature and Acronyms

Latin Letters and Acronyms

API	Active pharmaceutical ingredient
b	Crystal nucleation exponent (–)
B_i	Crystal nucleation rate (# m^{-3} min^{-1})
BLIC	Battery limits installed costs (GBP)
C_i	API concentration in product magma of MSMPR i (g mL^{-1})
$C_{i,sat}$	API saturation concentration at T_i (g mL^{-1})
C_0	Mother liquor API concentration of the fresh feed stream (g mL^{-1})
CapEx	Capital expenditure (GBP)
CC	Contingency costs (GBP)
CEPCI	Chemical engineering plant cost index
CPM	Continuous pharmaceutical manufacturing
E_{ag}	Crystal growth activation energy (J mol^{-1})
f	Correction factor in eq. 15
F_i	Volumetric flowrate of stream i (mL min^{-1})
F_0	Volumetric flowrate of the fresh feed stream (mL min^{-1})
FOB	Free-on-Board Costs (GBP)
g	Crystal growth exponent (–)
G_i	Crystal linear growth rate (m min^{-1})
IEC	Installed equipment costs (GBP)
k_{b0}	Pre-exponential factor for crystal nucleation (# m^{-3} min^{-1})
k_{g0}	Pre-exponential factor for crystal growth (m min^{-1})
k_v	Crystal volume shape factor (–)
L	Crystal characteristic length (m)
M_i	MSMPR slurry density (g mL^{-1})
MAT_{annual}	Annual material costs (GBP y^{-1})
MSMPR	Mixed suspension, mixed product removal crystallizer
N	Total number of MSMPRs in crystallization cascade
n	Exponent in eq. 15
n_i	Crystal population density (# m^{-3} m^{-1})

n_i^0	Nuclei population density (# m^{-3} m^{-1})
NPV	Net present value
ODE	Ordinary differential equation
$OpEx_{annual}$	Annual operating expenditure (GBP y^{-1})
P_j	Equipment purchase cost at capacity *j* (GBP)
PAT	Process Analytical Technology
PPI	Process piping and instrumentation costs (GBP)
Q_{API}	Plant API production capacity (kg y^{-1})
R	Universal gas constant (= 8.314 J mol^{-1} K^{-1})
r	Interest rate (%)
S_j	Capacity of equipment (varying units)
t	Plant operation lifetime (y)
T_i	Operating temperature of MSMPR *i* (°C)
$T_{i,opt}$	Operating temperature of MSMPR *i* (°C) corresponding to minimum total costs
$\boldsymbol{T_0}$	Vector of initial crystallizer temperatures (°C)
TPPC	Total physical plant cost (GBP)
$UTIL_{annual}$	Annual utilities costs (GBP y^{-1})
V_i	Volume of MSMPR *i* (mL)
$V_{i,opt}$	Volume of MSMPR *i* (mL) corresponding to minimum total costs
$V_{TOT,opt}$	Total volume of all crystallizers in series (mL) corresponding to minimum total costs
$Waste_{annual}$	Annual waste disposal cost (GBP y^{-1})
WC	Working capital costs (GBP)
WCC	Working capital and contingency costs (GBP)
Y_{cryst}	Crystallisation yield (%)

Greek Letters

ρ_{API}	API solid crystal density (g cm^{-3})
$\rho_{solvent}$	Mother liquor solvent density at T_i (g mL^{-1})
τ_i	Residence time in MSMPR *i* (min)
$\tau_{i,opt}$	Residence time in MSMPR *i* (min) corresponding to minimum total costs
$\boldsymbol{\tau_0}$	Vector of initial crystallizer residence times (h)
$\tau_{TOT,opt}$	Total cascade residence time (min) corresponding to minimum total costs

References

1. Poechlauer, P., Colberg, J., Fisher, E., Jansen, M., Johnson, M. D., Koenig, S. G., Lawler, M., Laporte, T., Manley, J., Martin, B., O'Kearney-McMullan, A. Pharmaceutical Roundtable Study Demonstrates the Value of Continuous Manufacturing in the Design of Greener Processes. *Org. Process Res. Dev.* **17,** 1472–1478 (2013).
2. Dallinger, D., Kappe, C. O. Why flow means green – Evaluating the merits of continuous processing in the context of sustainability. *Current Opinion in Green and Sustainable Chemistry* **7,** 6–12 (2017).
3. Schaber, S. D., Gerogiorgis, D. I., Ramachandran, R., Evans, J. M. B., Barton, P. I., Trout, B. L. Economic Analysis of Integrated Continuous and Batch Pharmaceutical Manufacturing: A Case Study. *Ind. Eng. Chem. Res.* **50,** 10083–10092 (2011).
4. Plumb, K. Continuous Processing in the Pharmaceutical Industry - Changing the Mind Set. *Chem. Eng. Res. Des.* **83,** 730–738 (2005).
5. Malet-Sanz, L., Susanne, F. Continuous Flow Synthesis. A Pharma Perspective. *J. Med. Chem.* **55,** 4062–4098 (2012).
6. Baumann, M., Baxendale, I. R. The Synthesis of Active Pharmaceutical Ingredients (APIs) Using Continuous Flow Chemistry. *Beilstein J. Org. Chem.* **11,** 1194–1219 (2015).
7. Porta, R., Benaglia, M., Puglisi, A. Flow Chemistry: Recent Developments in the Synthesis of Pharmaceutical Products. *Org. Process Res. Dev.* **20,** 2–25 (2015).
8. Britton, J., Raston, C. L., Planchestainer, M., Contente, M. L., Cassidy, J., Molinari, F., Tamborini, L., Raston, C. L. *et al.* Multi-step continuous-flow synthesis. *Chem. Soc. Rev.* **52,**

10159–10162 (2017).
9. Plutschack, M. B., Pieber, B., Gilmore, K., Seeberger, P. H. The Hitchhiker's Guide to Flow Chemistry. *Chemical reviews* **117,** 11796–11893 (2017).
10. Mascia, S., Heider, P. L., Zhang, H., Lakerveld, R., Benyahia, B., Barton, P. I., Braatz, R. D., Cooney, C. L., Evans, J. M. B., Jamison, T. F., Jensen, K. F., Myerson, A. S., Trout, B. L. End-to-end Continuous Manufacturing of Pharmaceuticals: Integrated Synthesis, Purification, and Final Dosage Formation. *Angew. Chemie-International Ed.* **52,** 12359–12363 (2013).
11. Adamo, A., Beingessner, R. L., Behnam, M., Chen, J., Jamison, T. F., Jensen, K. F., Monbaliu, J.-C. M., Myerson, A. S., Revalor, E. M., Snead, D. R., Stelzer, T., Weeranoppanant, N., Wong, S. Y., Zhang, P. On-Demand Continuous-Flow Production of Pharmaceuticals in a Compact, Reconfigurable System. *Science (80-.).* **352,** 61–67 (2016).
12. GSK. GSK invests a further S$77mil to enhance antibiotic manufacturing facility in Singapore | GSK Singapore. (2015). Available at: http://sg.gsk.com/en-sg/media/press-releases/2015/gsk-invests-a-further-s-77mil-to-enhance-antibiotic-manufacturing-facility-in-singapore/. (Accessed: 3rd February 2016)
13. Kuehn, S. E. Janssen Embraces Continuous Manufacturing for Prezista. *Pharmaceutical Manufacturing* (2015). Available at: http://www.pharmamanufacturing.com/articles/2015/janssen-embraces-continuous-manufacturing-for-prezista/. (Accessed: 5th October 2016)
14. Baxendale, I. R., Braatz, R. D., Hodnett, B. K., Jensen, K. F., Johnson, M. D., Sharratt, P., Sherlock, J.-P., Florence, A. J. Achieving continuous manufacturing: technologies and approaches for synthesis, workup, and isolation of drug substance. *J. Pharm. Sci.* **104,** 781–791 (2015).
15. Chen, J., Sarma, B., Evans, J. M. B., Myerson, A. S. Pharmaceutical Crystallization. *Cryst. Growth Des.* **11,** 887–895 (2011).
16. Zhang, D., Xu, S., Du, S., Wang, J., Gong, J. Progress of Pharmaceutical Continuous Crystallization. *Engineering* **3,** 354–364 (2017).
17. Rogers, A., Ierapetritou, M. Challenges and Opportunities in Pharmaceutical Manufacturing Modelling and Optimization. *Comput. Aided Chem. Eng.* **34,** 144–149 (2014).
18. Alvarez, A. J., Singh, A., Myerson, A. S. Crystallization of cyclosporine in a multistage continuous MSMPR crystallizer. *Cryst. Growth Des.* **11,** 4392–4400 (2011).
19. Power, G., Hou, G., Kamaraju, V. K., Morris, G., Zhao, Y., Glennon, B. Design and optimization of a multistage continuous cooling mixed suspension, mixed product removal crystallizer. *Chem. Eng. Sci.* **133,** 125–139 (2015).
20. Quon, J. L., Zhang, H., Alvarez, A., Evans, J., Myerson, A. S., Trout, B. L. Continuous crystallization of Aliskiren hemifumarate. *Cryst. Growth Des.* **12,** 3036–3044 (2012).
21. Morris, G., Power, G., Ferguson, S., Barrett, M., Hou, G., Glennon, B. Estimation of Nucleation and Growth Kinetics of Benzoic Acid by Population Balance Modeling of a Continuous Cooling Mixed Suspension, Mixed Product Removal Crystallizer. *Org. Process Res. Dev.* **19,** 1891–1902 (2015).
22. Ferguson, S., Morris, G., Hao, H., Barrett, M., Glennon, B. Characterization of the anti-solvent batch, plug flow and MSMPR crystallization of benzoic acid. *Chem. Eng. Sci.* **104,** 44–54 (2013).
23. Su, Q., Nagy, Z. K., Rielly, C. D. Pharmaceutical crystallisation processes from batch to continuous operation using MSMPR stages: Modelling, design, and control. *Chem. Eng. Process. Process Intensif.* **89,** 41–53 (2015).
24. Li, J., Trout, B. L., Myerson, A. S. Multistage Continuous Mixed-Suspension, Mixed-Product Removal (MSMPR) Crystallization with Solids Recycle. *Org. Process Res. Dev.* **20,** 510–516 (2016).
25. Park, K., Kim, D. Y., Yang, D. R. Operating Strategy for Continuous Multistage Mixed Suspension and Mixed Product Removal (MSMPR) Crystallization Processes Depending on Crystallization Kinetic Parameters. *Ind. Eng. Chem. Res.* **55,** 7142–7153 (2016).
26. Zhang, H., Quon, J., Alvarez, A. J., Evans, J., Myerson, A. S., Trout, B. Development of continuous anti-solvent/cooling crystallization process using cascaded mixed suspension, mixed product removal crystallizers. *Org. Process Res. Dev.* **16,** 915–924 (2012).

27. Gruber-Woelfler, H., Escribà-Gelonch, M., Noël, T., Maier, M. C., Hessel, V. Effect of Acetonitrile-Based Crystallization Conditions on the Crystal Quality of Vitamin D_3. *Chem. Eng. Technol.* **40,** 2016–2024 (2017).
28. Yang, Y., Nagy, Z. K. Combined Cooling and Antisolvent Crystallization in Continuous Mixed Suspension, Mixed Product Removal Cascade Crystallizers: Steady-State and Startup Optimization. *Ind. Eng. Chem. Res.* **54,** 5673–5682 (2015).
29. Yang, Y., Nagy, Z. K. Advanced control approaches for combined cooling/antisolvent crystallization in continuous mixed suspension mixed product removal cascade crystallizers. *Chem. Eng. Sci.* **127,** 362–373 (2015).
30. Vetter, T., Burcham, C. L., Doherty, M. F. Regions of attainable particle sizes in continuous and batch crystallization processes. *Chem. Eng. Sci.* **106,** 167–180 (2014).
31. Wong, S. Y., Tatusko, A. P., Trout, B. L., Myerson, A. S. Development of continuous crystallization processes using a single-stage mixed-suspension, mixed-product removal crystallizer with recycle. *Cryst. Growth Des.* **12,** 5701–5707 (2012).
32. Acevedo, D., Yang, Y., Warnke, D. J., Nagy, Z. K. Model-Based Evaluation of Direct Nucleation Control Approaches for the Continuous Cooling Crystallization of Paracetamol in a Mixed Suspension Mixed Product Removal System. *Cryst. Growth Des.* **17,** 5377–5383 (2017).
33. Yang, X., Acevedo, D., Mohammad, A., Pavurala, N., Wu, H., Brayton, A. L., Shaw, R. A., Goldman, M. J., He, F., Li, S., Fisher, R. J., O'Connor, T. F., Cruz, C. N. Risk Considerations on Developing a Continuous Crystallization System for Carbamazepine. *Org. Process Res. Dev.* **21,** 1021–1033 (2017).
34. Agnew, L. R., McGlone, T., Wheatcroft, H. P., Robertson, A., Parsons, A. R., Wilson, C. C. Continuous Crystallization of Paracetamol (Acetaminophen) Form II: Selective Access to a Metastable Solid Form. *Cryst. Growth Des.* **17,** 2418–2427 (2017).
35. Su, Q., Rielly, C. D., Powell, K. A., Nagy, Z. K. Mathematical modelling and experimental validation of a novel periodic flow crystallization using MSMPR crystallizers. *AIChE J.* (2016). doi:10.1002/aic.15510
36. Powell, K. A., Saleemi, A. N., Rielly, C. D., Nagy, Z. K. Periodic steady-state flow crystallization of a pharmaceutical drug using MSMPR operation. *Chem. Eng. Process. Process Intensif.* **97,** 195–212 (2015).
37. Tahara, K., O'Mahony, M., Myerson, A. S. Continuous spherical crystallization of albuterol sulfate with solvent recycle system. *Cryst. Growth Des.* **15,** 5155–5156 (2015).
38. Li, J., Lai, T. C., Trout, B. L., Myerson, A. S. Continuous Crystallization of Cyclosporine: the Effect of Operating Conditions on Yield and Purity. *Cryst. Growth Des.* **17,** 1000–1007 (2017).
39. Ferguson, S., Ortner, F., Quon, J., Peeva, L., Livingston, A., Trout, B. L., Myerson, A. S. Use of continuous MSMPR crystallization with integrated nanofiltration membrane recycle for enhanced yield and purity in API crystallization. *Cryst. Growth Des.* **14,** 617–627 (2014).
40. Vartak, S., Myerson, A. S. Continuous Crystallization with Impurity Complexation and Nanofiltration Recycle. *Org. Process Res. Dev.* **21,** 253–261 (2017).
41. Hou, G., Power, G., Barrett, M., Glennon, B., Morris, G., Zhao, Y. Development and characterization of a single stage mixed-suspension, mixed-product-removal crystallization process with a novel transfer unit. *Cryst. Growth Des.* **14,** 1782–1793 (2014).
42. Acevedo, D., Peña, R., Yang, Y., Barton, A., Firth, P., Nagy, Z. K. Evaluation of mixed suspension mixed product removal crystallization processes coupled with a continuous filtration system. *Chem. Eng. Process. Process Intensif.* **108,** 212–219 (2016).
43. Wang, J., Lakerveld, R. Integrated solvent and process design for continuous crystallization and solvent recycling using PC-SAFT. *AIChE J.* **64,** 1205–1216 (2018).
44. Galan, K., Eicke, M. J., Elsner, M. P., Lorenz, H., Seidel-Morgenstern, A. Continuous preferential crystallization of chiral molecules in single and coupled mixed-suspension mixed-product-removal crystallizers. *Cryst. Growth Des.* **15,** 1808–1818 (2015).
45. Kwon, J. S.-I., Nayhouse, M., Christofides, P. D., Orkoulas, G. Modeling and control of crystal shape in continuous protein crystallization. *Chem. Eng. Sci.* **107,** 47–57 (2014).
46. Kwon, J. S.-I., Nayhouse, M., Orkoulas, G., Christofides, P.D., Crystal shape and size control

using a plug flow crystallization configuration. *Chem. Eng. Sci.* **119,** 30–39 (2014).
47. Lai, T.-T. C., Cornevin, J., Ferguson, S., Li, N., Trout, B. L., Myerson, A. S. Control of Polymorphism in Continuous Crystallization via Mixed Suspension Mixed Product Removal Systems Cascade Design. *Cryst. Growth Des.* **15,** 3374–3382 (2015).
48. Lai, T.-T. C., Ferguson, S., Palmer, L., Trout, B. L., Myerson, A. S. Continuous Crystallization and Polymorph Dynamics in the l -Glutamic Acid System. *Org. Process Res. Dev.* **18,** 1382–1390 (2014).
49. Yang, Y., Song, L., Gao, T., Nagy, Z. K. Integrated Upstream and Downstream Application of Wet Milling with Continuous Mixed Suspension Mixed Product Removal Crystallization. *Cryst. Growth Des.* **15,** 5879–5885 (2015).
50. Singhvi, N., Koo, M., Kyle, A. *Systemic Hypertension Market and Forecast Analyst to 2023 | Report Store | Pharma intelligence | Informa*. (2017).
51. Statista. *OTC Pharmaceuticals - United States*. (2017).
52. Jolliffe, H. G., Gerogiorgis, D. I. Technoeconomic Optimization of a Conceptual Flowsheet for Continuous Separation of an Analgaesic Active Pharmaceutical Ingredient (API). *Ind. Eng. Chem. Res.* **56,** 4357–4376 (2017).
53. Jolliffe, H. G., Gerogiorgis, D. I. Technoeconomic optimisation and comparative environmental impact evaluation of continuous crystallisation and antisolvent selection for artemisinin recovery. *Comput. Chem. Eng.* **103,** 218–232 (2017).
54. Jolliffe, H. G., Diab, S., Gerogiorgis, D. I. Nonlinear optimisation via explicit NRTL model solubility prediction for antisolvent mixture selection in artemisinin crystallisation. *Org. Process Res. Dev.* **22,** 40–53 (2018).
55. Dencic, I., Ott, D., Kralisch, D., Noel, T., Meuldijk, J., de Croon, M., Hessel, V., Laribi, Y., Perrichon, P. Eco-efficiency Analysis for Intensified Production of an Active Pharmaceutical Ingredient: A Case Study. *Org. Process Res. Dev.* **18,** 1326–1338 (2014).
56. Teoh, S. K., Rathi, C., Sharratt, P. Practical Assessment Methodology for Converting Fine Chemicals Processes from Batch to Continuous. *Org. Process Res. Dev.* **20,** 414–431 (2015).
57. Diab, S., Gerogiorgis, D. I. Technoeconomic evaluation of multiple mixed suspension-mixed product removal (MSMPR) crystallizer configurations for continuous cyclosporine crystallization. *Org. Process Res. Dev.* **21,** 1571–1587 (2017).
58. Jolliffe, H. G., Gerogiorgis, D. I. Plantwide Design and Economic Evaluation of Two Continuous Pharmaceutical Manufacturing (CPM) Cases: Ibuprofen and Artemisinin. *Comput. Chem. Eng.* **91,** 269–288 (2016).
59. Atwood, J. L. Separation of Active Pharmaceutical Ingredients (APIs) from excipients in pharmaceutical formulations. *Cryst. Growth Des.* **15,** 2874–2877 (2015).
60. Granberg, R. A., Rasmuson, Å. C. Crystal growth rates of paracetamol in mixtures of water + acetone + toluene. in *AIChE Journal* **51,** 2441–2456 (Wiley Subscription Services, Inc., A Wiley Company, 2005).
61. Chianese, A., Kramer, H. J. M. *Industrial Crystallization Process Monitoring and Control*. *Industrial Crystallization Process Monitoring and Control* (Wiley-VCH Verlag GmbH & Co. KGaA, 2012). doi:10.1002/9783527645206
62. Woods, D. R. *Rules of Thumb in Engineering Practice*. (Wiley, 2007).
63. ProMinent. Solenoid Driven Metering Pumps. (2015). Available at: https://www.prominent.co.uk/en/Products/Products/Metering-Pumps/Solenoid-Driven-Metering-Pumps/pg-solenoid-driven-metering-pumps.html. (Accessed: 8th March 2016)
64. Couper, J. R. *Process Engineering Economics*. (CRC Press, 2003).
65. Shoham Patrascu, M., Barton, P. I. Dynamic Optimization of Continuous Manufacturing of Pharmaceuticals. *Comput. Aided Chem. Eng.* **40,** 2803–2808 (2017).
66. Wu, H., Dong, Z., Li, H., Khan, M. An Integrated Process Analytical Technology (PAT) Approach for Pharmaceutical Crystallization Process Understanding to Ensure Product Quality and Safety: FDA Scientist's Perspective. *Org. Process Res. Dev.* **19,** 89–101 (2015).

TABLE OF CONTENTS GRAPHIC